IRON ABUNDANCE ESTIMATION OF THE LUNAR SURFACE USING VIS-NIR SPECTROMETERS ON-BOARD CHANDRAYAAN-1. M. Bhatt, U. Mall and R. Bugiolacchi, Max Planck Institute for Solar System Research, 37191, Katlenburg-Lindau, Germany (bhatt@mps.mpg.de).

Introduction: Iron is a key element to understand the origin and evolution of planetary surfaces. The indirect measurement of the iron content in terms of the FeO weight present (wt%) is possible by measuring the absorption band parameters of visible/near-infrared (VIS-NIR) reflectance spectra in the wavelength range 0.4 to 2.5 µm . The principle absorption characteristics of lunar reflectance spectra in the VIS-NIR wavelength range are due to ferrous iron (Fe^{+2}) transition at the different crystallographic sites of the minerals [1]. However, the effects of space weathering weaken the mineral absorption band depth and redden the spectral continuum slope, thus making the detection and quantification of its constituent minerals (iron bearing silicates) challenging [2, 3]. Various attempts have been made to decouple the spectral effects of mineral composition from the surface maturity by utilizing the 1-µm absorption band parameters for Clementine and telescopic datasets [e.g., 4–8].

Our method is based on the 2-µm absorption parameters. We have applied this method to the Copernicus crater from nearside and Mare Moscovience basin from farside of the Moon. We have also compared our results with those published from the Clementine mission.

Data-sets and data-processing: In this study, we have employed data from the Infra-red Spectrometer, SIR-2 [9] and Moon Mineralogy Mapper (M^3) [10] on-board Chandrayaan-1 [11]. Copernicus crater was sampled by SIR-2 orbits 1095 and 1096 with orbit 1096 crossing the crater's central peak. SIR-2 orbits 606, 610 and 614 crossed Mare Moscoviense and surroundings. We selected M^3 product IDs corresponding to SIR-2 orbits to ensure that both data-sets are photometrically comparable. FeO wt% maps from the Clementine mission have been used to compare results.

The SIR-2 raw data are converted to calibrated radiance by subtracting dark and bias and by using the instrument's sensitivity function. The calibrated radiance values are converted into absolute reflectance by dividing through a standard solar irradiance spectrum and the cosine of the incidence angle. We have obtained the "apparent reflectance" for the M^3 data by dividing radiance by the standard solar irradiance and the cosine of the incidence angle.

Iron abundance maps of Mare Moscoviense and Copernicus: A total of five major compositional units have been identified from the Mare Moscoviense region [12, 13] and at least three different volcanic eruptive events were observed. The different volcanic units show variations in their FeO and TiO_2 wt% abundances. A wide difference in TiO_2 and FeO values has been observed across Mare Moscoviense soils according to [14] Clementine-derived iron map. Figure 1 shows these variations in terms of FeO wt% estimation maps of SIR-2 and M^3. SIR-2 orbits 606 and 610 show the area within Mare Moscoviense while orbit 614 falls outside Mare Moscoviense. The youngest mare unit in the basin exhibits the highest FeO wt% (between 22-25) in Figure 1 for SIR-2 orbit 606, 610 and corresponding M^3 orbits. The second unit has a surface composition with FeO wt% ranging between 18-20 and overlain by the youngest unit.

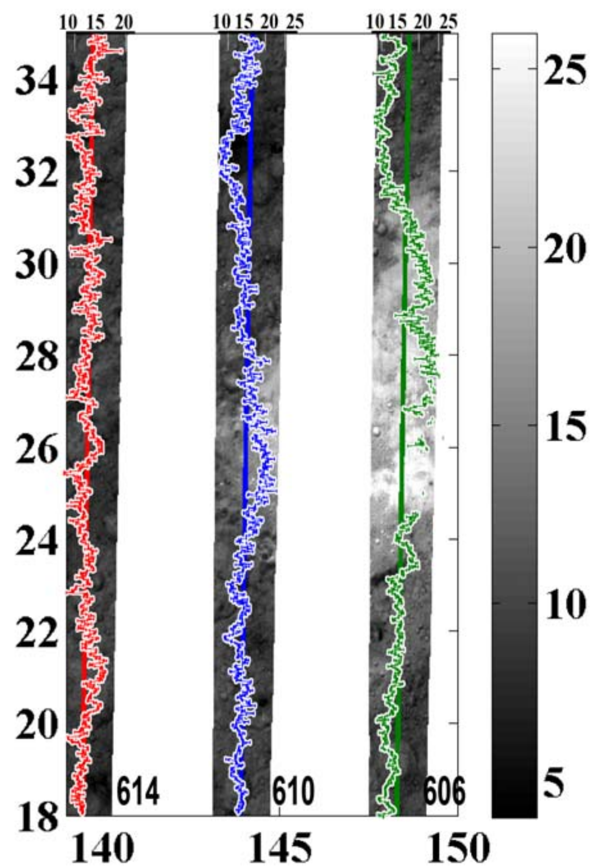

Figure 1: Iron abundance maps for Mare Moscoviense and surroundings, derived from SIR-2 and M3 orbit.

This unit may represent highland-contaminated mare soil. The ancient mare unit is mapped north and south of SIR-2 orbits 606 and 610. This unit is more heavily cratered and shows low FeO wt%, in the range 8-12. The average FeO wt% for the SIR-2 orbit 614 is about 15. [14] suggested the presence of cryptomare deposits between the inner and outer rings of the Mare Moscoviense basin. SIR-2 orbit 614 falls within the middle and outer rings. A detailed spectral study of SIR-2 orbit 614 may help us detecting cryptomare deposits in this region. Our results are in good agreement with [14]; however, FeO wt% ranges are higher by 2-3 wt% when compared to the Clementine iron abundance map from [14].

Copernicus is classified as a highland crater and located within a highly complex geological region [15]. Copernicus central peak is identified as olivine rich from previous studies [e.g., 15–19]. Our FeO wt% abundance estimation algorithm is based on detecting pyroxene absorption bands in the 2-μm region and do not account for iron contained in minerals with prominent absorption bands with expression only in the 1-μm region. Therefore, our method may show low accuracy for olivine rich areas. We selected Copernicus crater to check for the discrepancies present between iron abundance estimation maps derived from SIR-2 and M^3 orbits utilizing the 2-μm absorption band parameters with Clementine iron abundance maps are based on [5] algorithm. Figure 2 shows the iron abundance estimation for SIR-2 as a line plot on top of the iron abundance estimation map from M^3 generated in the same way as the SIR-2 data. The average FeO wt% from Figure 2 is about 10-12 wt% within Copernicus and ranges between 10 to 20 wt% for the SIR-2 data. We observed that all the three data-sets give the average FeO wt% for Copernicus crater in the same range; however, overall FeO wt% values vary significantly. The area outside the crater is mapped as iron-rich with FeO ranging between 20-25 wt% by Clementine while the same area is mapped within the range of 15-20 wt% by M^3. SIR-2 predicts an average of 15 wt% FeO for the same area. Figure 2 shows that the overall FeO variation trends are similar but the absolute values do not match. A careful investigation will be carried out to address this problem. Figure 2 shows that our method is less sensitive to the topography than the method based on Clementine UV-Visible band ratio.

Summary: Our comparative analysis shows that iron abundance estimated using the 2-μm absorption band parameters shares the same trend as the FeO wt% map derived for Clementine data and can be used effectively to generate global FeO wt% maps of the lunar surface. Our first attempt to correlate SIR-2, M^3, and Clementine iron maps can be deemed successful and further refinements will be carried out when fully calibrated SIR-2 and M^3 data sets will become available.

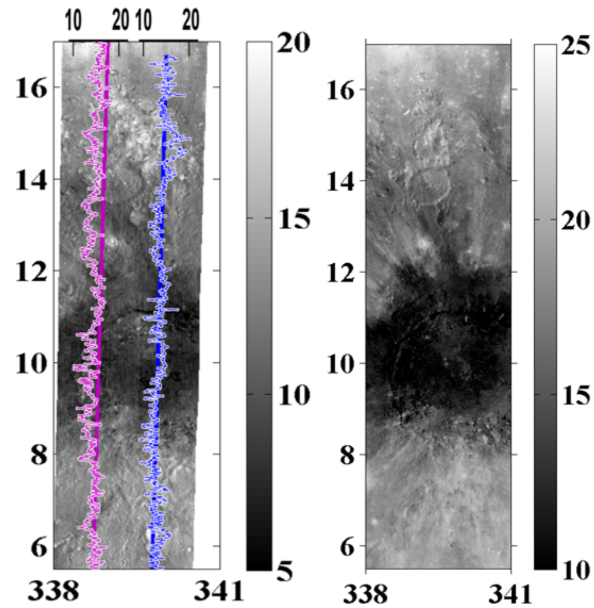

Figure 2: Iron abundance maps for Copernicus. The SIR-2 and M3 maps based on 2-μm absorption band parameters are shown in left panel and the Clementine map is shown in right panel.

References: [1] Burns R., Remote geochemical analysis: Elemental and mineralogical composition, (1993). [2] Fischer E.M. and Pieters C.M., (1994) *Icarus*, 111, 475–488. [3] Fischer E.M. and Pieters C.M., (1996) *JGR*, 101, 2225–2234. [4] Lucey P.G. et al., (1995), *Science*, 268, 1150–1153. [5] Lucey P.G. et al., (1998) *JGR*, 103, 3679-3699. [6] Le Mouélic S. et al., (2000) *JGR*, 105, 9445–9456. [7] Shkuratov Y.G. et al., (2005) *PlanSS*, 53, 1287–1301. [8] Wöhler C. et al., (2011) *PlanSS*, 59, 92–110. [9] Mall U. et al., (2009) *Current Science*, 96, 506–511. [10] Pieters C. et al., (2009) *Current Science*, 96, 500–505. [11] Goswami J. and Annadurai M., (2009) *Current Science*, 96, 486–491. [12] Kramer G.Y. et al., (2008) *JGR (Planets)*, 113, E01002. [13] Gillis J. J. (1998) *PhD thesis*, Rice Univ., Houston, Texas. [14] Gillis J.J. et al. (2006) *LPSC*, 37, 2454. [15] Pieters C.M., (1982) *Science*, 215, 59–61. [16] Lucey P.G. et al., (1991) *GRL*, 18, 2133–2136. [17] Mouélic S.L. and Langevin Y., (2001) *Planss*, 49, 65–70. [18] Matsunaga T. et al., (2008) *GRL*, 35, L23201. [19] Bugiolacchi R. et al., (2011) *Icarus*, 213, 43–63.